

IMPROVED MIGRATIONS IN LATERALLY VARYING MEDIA, WIND RIVER,  
WYOMING

Heloise Bloxsom Lynn, Laura Gagnon, and Don Seeburger

Abstract

A COCORP dataset from the south end of the Wind River Mountains, Wyoming, showing the Wind River thrust juxtaposing Precambrian crystalline rocks and Mesozoic sediments, was the input to a series of migrations, wherein the velocity model was a function of depth and lateral distance. A well 1.6 km from the line provided constraints for the  $V(x,z)$  model input to the 45 degree w-finite difference program. Too high velocities in the near surface and in the Mesozoic-Precambrian transition zone produced "smiles" in the migrated sections (classic overmigration). The "smiles" observed in undermigrated sections were attributed to pullup in z caused by unusually slow near surface and fault zone velocities. The two best velocity models were used to migrate a larger, composite dataset of 470 traces (31.4 km) - 6 seconds. The results were interpreted geologically as follows: (1) The thickness of the Wind River thrust zone varies with depth (0-~3 km depth: 0.25-1.0 km thick; 3-7 km: ~1.5 km thick; 7-10 km: imbricate thrusting is the dominant feature; +10 km: ~2 km thick). (2) At least three subsidiary (imbricate) thrusts are seen between 4 and 9 km depth in the sedimentary sequence. (3) The dip angle of the thrust fault changes from 30 degrees to 0 degrees where it passes upward from Precambrian crystalline rock to sedimentary rock. The difference in rock properties (strength, anisotropy)

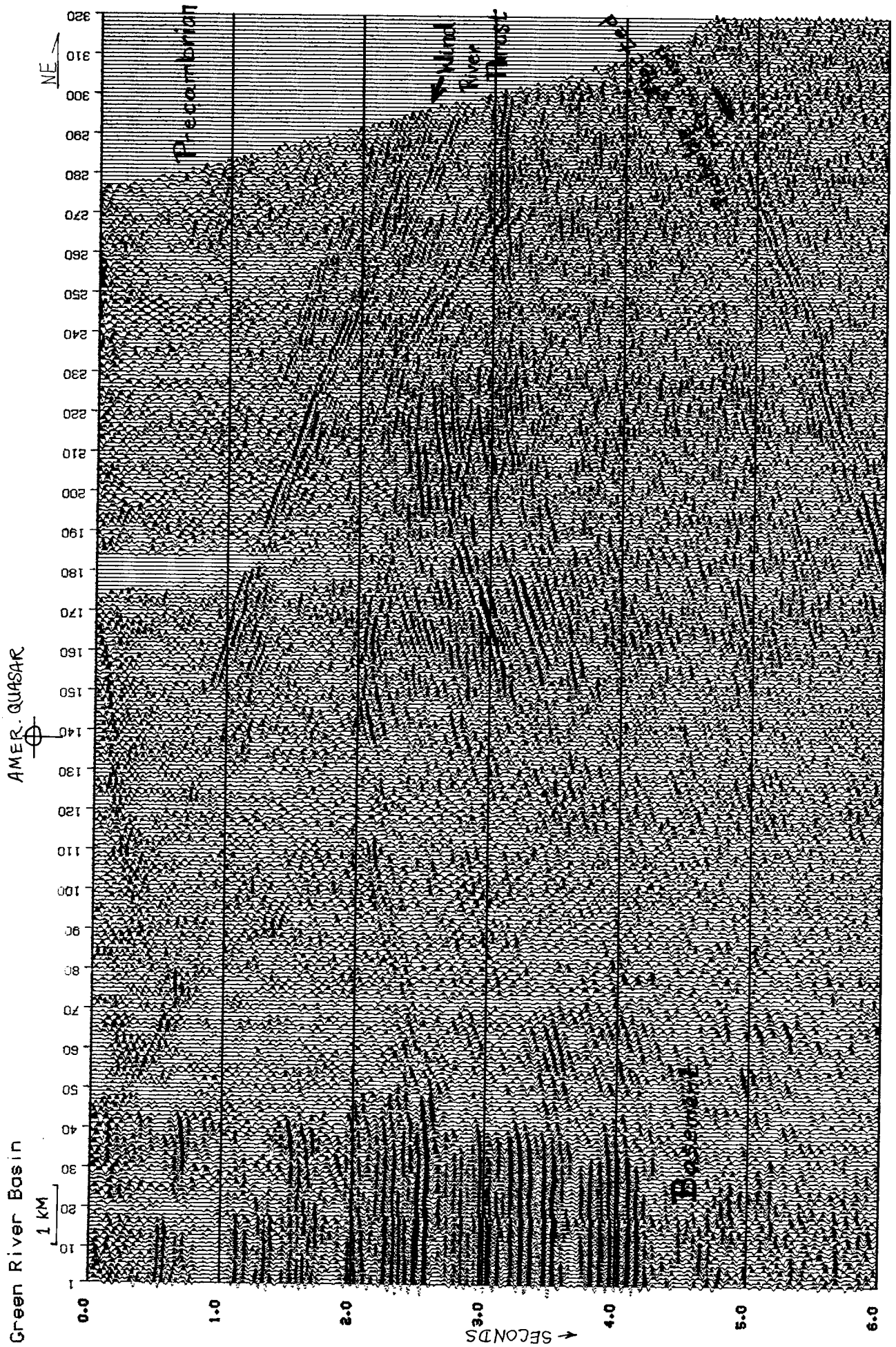
between a layered sedimentary sequence and Precambrian crystalline basement may explain the change in thrust angle.

### Introduction

Migrations in laterally varying media using the 45 degree w-finite difference algorithm have been discussed in SEP-15. Some migrations used geologically-derived earth models ("Applications and Comparisons of the Frequency Domain and the Finite Difference Migration Algorithms") and others used seismic-interval velocity models ("Steeply Faulted Regions, Artifacts, and Stability in the 45 w-Finite Difference Algorithm"). The general appearance of these "depth migrations," especially the effect of velocity upon wavelength (in z) has also been examined. The migrations with geologically based velocity models yielded more reasonable and believable migrated sections. Migrations should use earth velocities, not interval velocities (calculated by Dix's equation), when it is clear geologically that the interval velocities are inaccurate. Since SEP-15's publication, well data in this area has become available; this new data has provided important constraints on the earth model  $[V = V(x,z)]$ .

Figure 1 shows the base map for the input dataset(s). Figure 2 is the input time section (stations 229-389, line 1). The field, recording, and processing parameters for this line are given in the appendix. Note the Tertiary-Mesozoic sedimentary section of the Green River Basin on the left, the Wind River thrust (along arrows), and the Precambrian overthrust section.

FIGURE 2.--Unmigrated time section input to the migrations (stations 229-398, line 1). Trace spacing is 67 meters; numbers on top are trace numbers for this subset of line 1. This dataset is 21 km long. (~1:1 display of data.)



Well data information on V(x,z)

Well data and synthetic seismograms from the American Quasar Skinner Federal No. 1, 1.6 km (1 mile) north of line 1, (see Figure 1) were presented in "Analysis and Interpretation of COCORP Line 1, Wind River Uplift, Wyoming" (Hayes, 1977). He worked with unmigrated data. The well's projected location is trace 138 of the dataset (Figure 2). At the tiepoint, the well helped delineate a Tertiary sediment wedge, its (possible) velocity, the Precambrian velocity, the fault zone's velocity and depth, and the Mesozoic sediments' velocities (see Figure 3). The radical lateral variation in velocity encountered between traces 30-140 (Figure 2) invalidates the assumptions of CDP=CMP and hyperbolic events; the hyperbolic stack of CMP data, even with residual statics applied, degrades data quality. Thus, the well provides valuable information about the subsurface.

The well encountered the following formations and faults at these depths:

	DEPTH
Tertiary sediments	0 km
Precambrian	0.15
Fault	3.08
Cretaceous	3.08
Cretaceous Frontier	4.1
Fault	4.26
Tertiary Fort Union	4.26
Cretaceous Mesa Verde	4.27
T.D.	4.51

Note repeated section:  
older sedimentary rocks are  
thrust over younger rock.

TABLE 1.--American Quasar well information (from Hayes, 1977)

Prior to well control, the following reflections had been tentatively identified on the unmigrated section, based upon reflector strength and the overall trend of structure:

Tertiary sediments	0 sec
Top of Precambrian	0.167 sec
Top of Fault zone	0.75 sec
Rocks within fault zone (Pc? Mz?)	.75-1.1 sec

*[Is this zone the repeated Cretaceous section from 3.08-4.26 km? Or is this zone a fractured Precambrian region with lower (higher?) velocities?]*

Bottom of Fault zone	1.1 sec
Mz rocks below fault zone	below 1.1 sec

TABLE 2.-- First attempt to identify reflectors

However, when correlating the apparent traveltimes with well depths, velocities within the Precambrian were calculated to be unacceptably large (~10 km/s). Therefore, the data were re-examined. In the well, the unfractured Precambrian section above .85 sec has velocities of 5.9 to 6.1 km/s (Figure 3). The sonic log indicates a decrease in velocity (from 5.9 km/s to 4.8 km/s) at .85 to .95 sec. The average velocity in this "fractured" fault zone of Precambrian rock is ~5.5 km/s. The maximum fracturing (or porosity) probably occurs at the minimum velocity recorded (4.8 k/s) at .95 sec.

There are reflections on the synthetic seismograms (Figure 3) directly above the Precambrian/Cretaceous event (1.1 sec).

# SONIC VELOCITY [FT/S]      SYNTHETIC SEISMOGRAMS

8-16 HZ      6-32 HZ

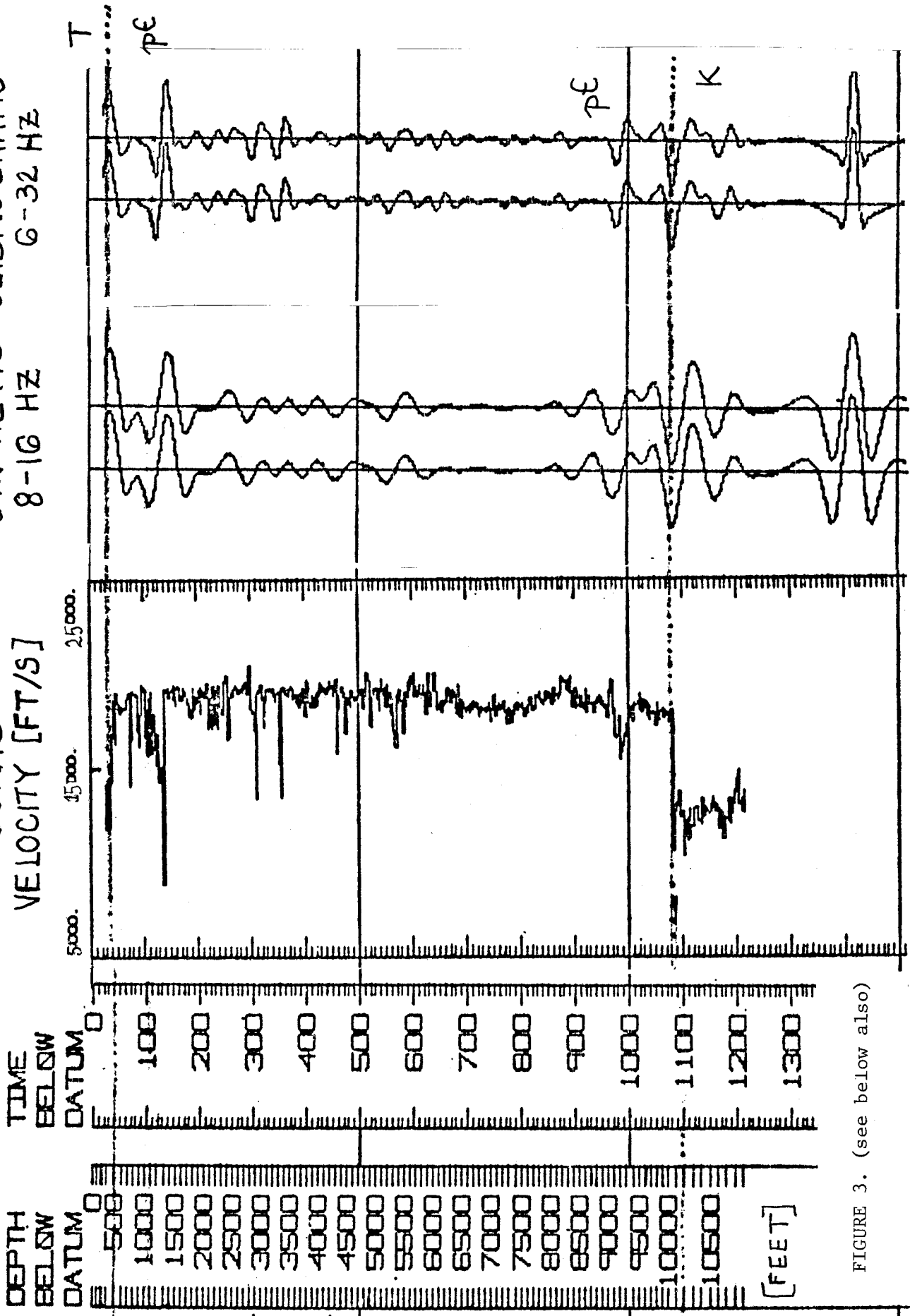


FIGURE 3. (see below also)

# SYNTHETIC SEISMOGRAMS

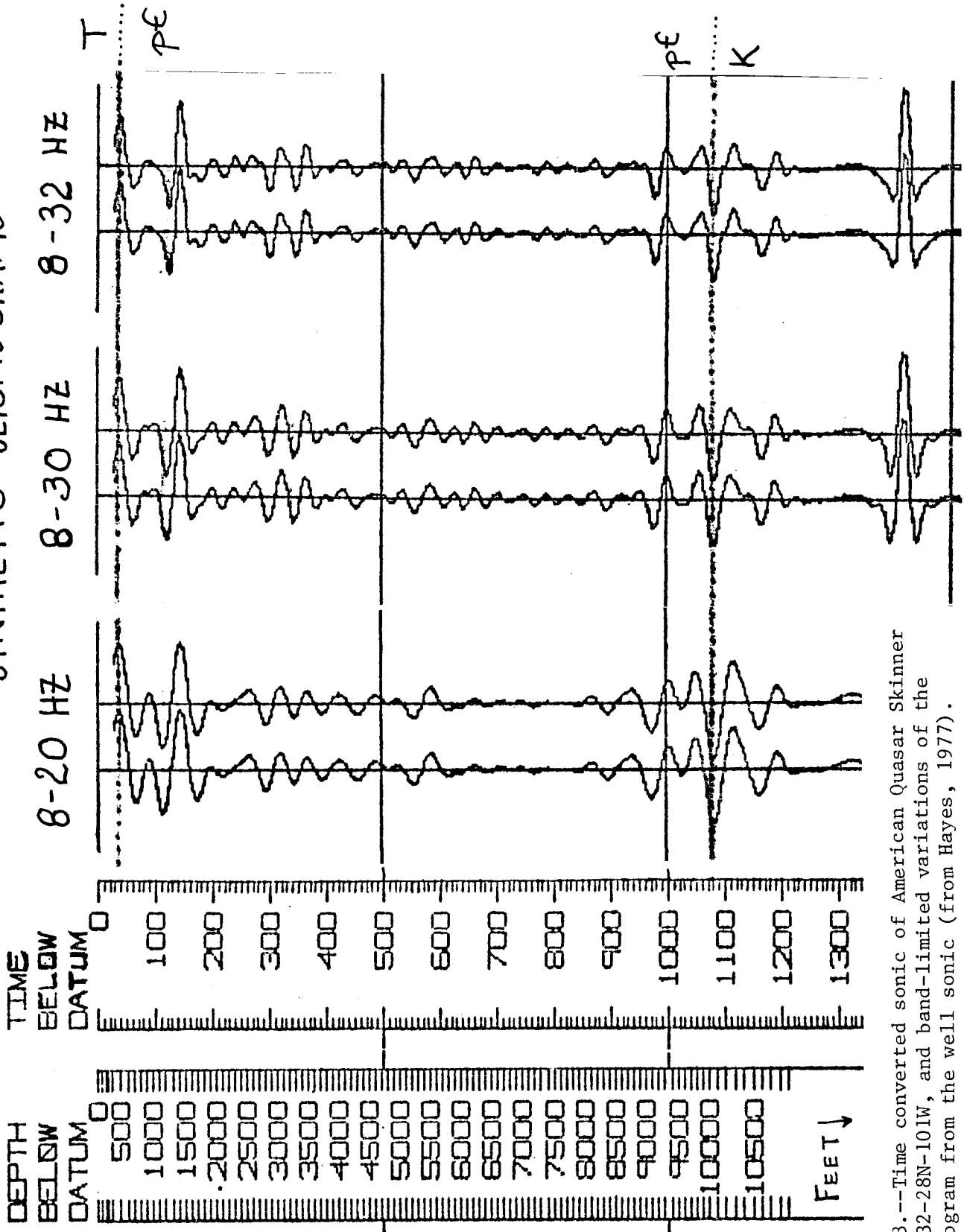


FIGURE 3.--Time converted sonic of American Quasar Skinner Federal No. 1, 32-28N-101W, and band-limited variations of the synthetic seismogram from the well sonic (from Hayes, 1977).

The frequency content of the synthetic seismogram plays quite an obvious role in determining the time of arrival and character of the reflections. The reflection at .95 sec on the 8-16 Hz synthetic is interpreted as the composite reflection from the high velocity top of the fault zone (5.98 k/s) and the low velocity (4.8 k/s) fractured zone in the middle of the fault zone. There are corresponding (low amplitude) reflections at those times on the section. This suggests that reflections at .95 and 1.1 sec represent the top and bottom of a fractured Precambrian rock fault zone about 600 m thick (2000 feet), wherein Precambrian crystalline rock has been crushed and ground due to thrusting. Reflector identification was then redone:

	<u>2-way time (sec)</u>	<u>Quasar well velocity (k/s)</u>	<u>Depth (km)</u>
Base of Tertiary	0.167	Tertiary: 4.0(?)	.15
Precambrian	.167-.95	Max Pc: 6.09 or Unfractured Pc: 5.84	.15-2.5
(Fractured) Pc rock thrust zone	.95-1.1	Top of fault zone: 5.97 Av. fault zone: 5.46 Min. vel. in fault zone: 4.8 at 2.74 km depth	2.5-3.08
Cretaceous (repeated section)	1.1-1.411	Top: ~3.8	3.08-4.26
Fault (within Mz section)	~1.4	?	4.26
Tertiary and Cretaceous	below ~1.4	?	4.26-4.505

TABLE 3.--Reflector identification and condensed well information (modified from Hayes, 1977)



Table 3 was made after several trial and error migrations. Some of those runs ignored the ~.6 km thick low velocity Precambrian fault zone; overmigrations resulted.

The near surface Tertiary wedge may become as thick as 900 m at trace 70 (see Figure 2), while having zero thickness 1.5 km to the SW and zero thickness 8 km to the NE. This represents a significant lateral velocity variation. However, the velocity of the Tertiary wedge is ambiguous. Using the Tertiary thickness found in the well and the reflection picked using both a near trace stack and the final stack, an average interval velocity of 1.8 k/s is calculated.

$$2 (0.15 \text{ km} ) / 0.167 \text{ sec} = 1.8 \text{ km/s}$$

Uncertainty in the velocity of this wedge has caused most of the problems in trying to migrate this dataset. Tertiary velocity was not adequately measured in the Quasar well (see Figure 3). If the "data" from the sonic log can be believed, the velocity of the base of the Tertiary is ~4.0 km/s. However, from the Pan American State of Wyoming No. 1 at the beginning of line 1 (~40 km away), the near surface Tertiary velocity is known to be 2.8-3.0 k/s. Therefore, possible interval velocities for the Tertiary on our dataset range from 1.8 k/s to 4 k/s.

## Migrations

1) Description of well-data constrained migrations. Model 4a (Figure 4a) shows a thin wedge of Tertiary sediments (using the Tertiary velocity seen in the well at the beginning of the line), and a thick Precambrian wedge and fault zone. Velocities in the Precambrian changed vertically from 5.6 to 6.2 km/s, while those in the repeated sedimentary sequence (or "transition zone") were slightly lower than Precambrian velocity (4.1-6.0 km/s). Overmigration of the sediments underlying the fault zone (trace 50-130) produced "smiles" at the left of the section between traces 1-30 at 4-6 km and 7-8 km depth (Figure 5). This overmigration resulted from too high velocities in the repeated section (measured to be ~3.8 k/s at the well's tiepoint). This overmigration suggests that the repeated section does not have such intensive secondary silicification or cementation that near-Precambrian velocities are reached.

Model 2 (Figure 4b) had less Precambrian rock, and combined the Tertiary and the transition zone into a more linear center zone. Significantly lower Tertiary velocities, lower sediment velocities, and higher Precambrian velocities were used. This model attempted to remove the half circles discussed above. Here, the model's center zone represents the fractured Precambrian fault zone, not the repeated Mesozoic section. Note that in these migrations we alternate between modeling the fractured Precambrian rock fault zone, and the repeated Mesozoic section. In some of these early migrations, we

became confused as to which had the greater effect upon the migration, and thus, which we should model. (We also found that if one cannot describe several laterally varying zones accurately, one may be better off just lumping them all together and describing the overall effect.) The "smiles" seen in the opposite direction on the output migrated section (Figure 6) are attributed not to overmigration but to pullup in  $z$  caused by too low velocities in the model's center zone.

Taking into account both of the above types of failures, a new model (Figure 7) was constructed. The Tertiary sediment wedge was thickened slightly (as suggested by the unmigrated data), the fault zone was thinned with an accompanying thin Precambrian wedge. Velocities were lowered slightly in the Tertiary and Precambrian, and lowered significantly in the fault zone. Model 7b has 8% slower Mesozoic velocities than Model 7a; otherwise, the two are identical.

The migrations (Figure 8, 9) using this model are better than Figs. 5-12. The sections are somewhat undermigrated---there are some pullups in  $z$  in the Mesozoic sediments after 9 km depth.

A model that more exactly conformed in structure to well data is shown next (Model 10a). This model is adapted from Figure 7. The fault zone was tied to well data so that the upper and lower horizons conformed to depths given in Hayes' paper. A thin fault zone (fractured Precambrian rock) thickening at 3.5 km depth was chosen as the most reasonable structure seen on the unmigrated data. We wanted to test the hypothesis that lower velocities might exist within the fractured Precam-

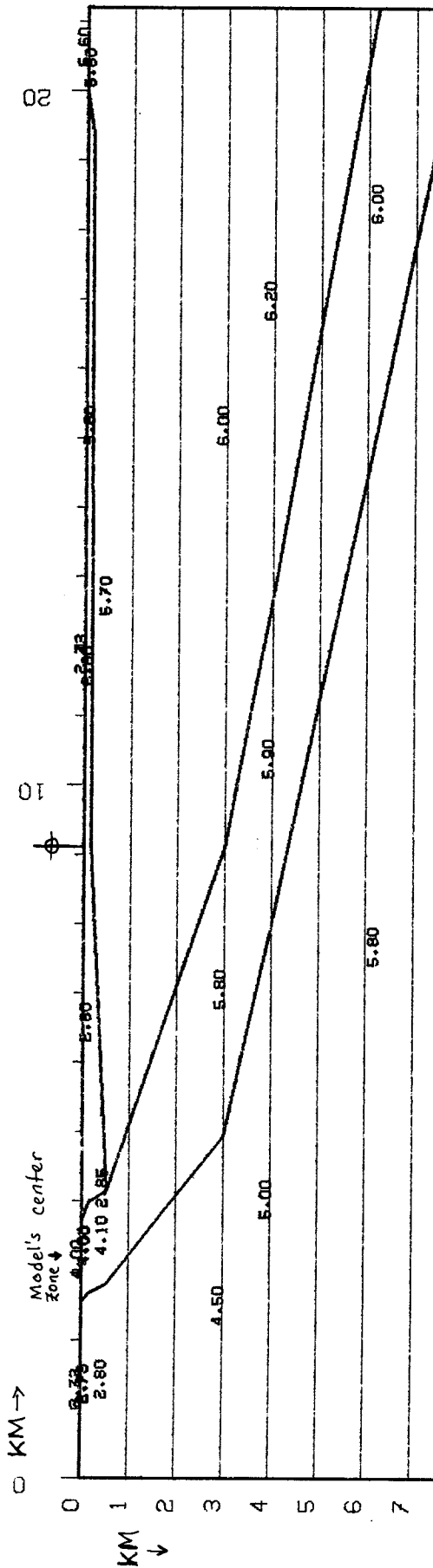
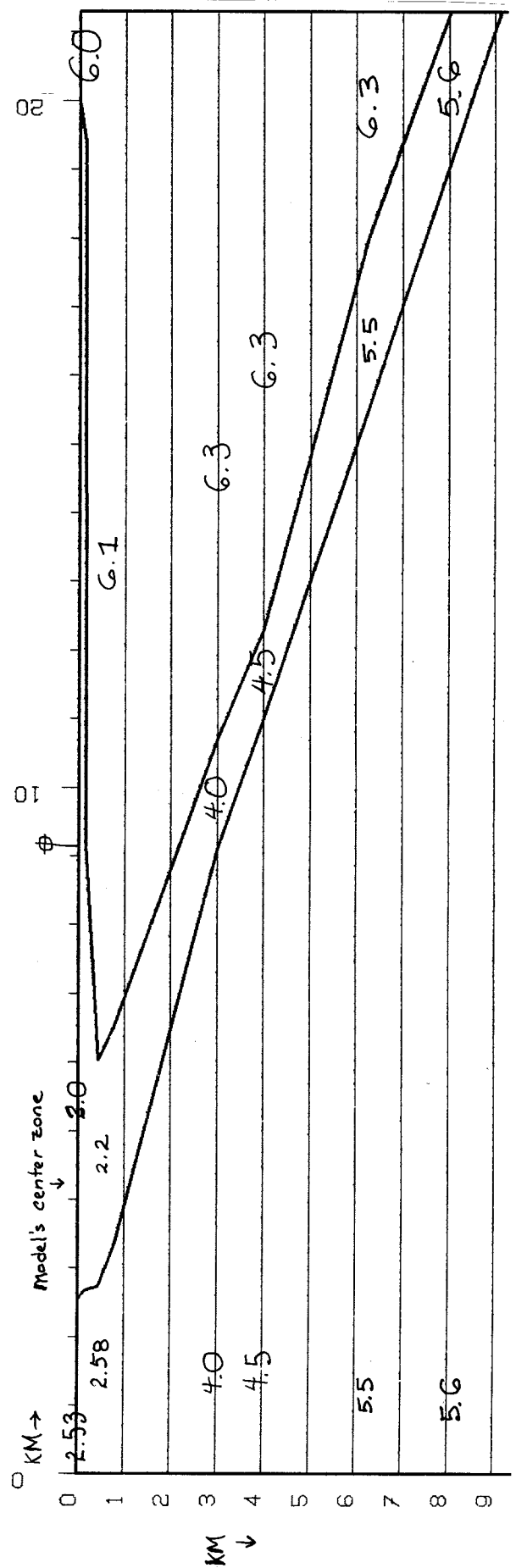


FIGURE 4.--Model 4a (above): The velocities are too high in the model's center zone (repeated Mesozoic section). From 0.5 - 6.0 km depth, the velocities are 4.1 - 6.0 k/s. Compaction and overburden pressure did not increase the repeated section's velocities up to ~5 - 5.5 k/s. The result is Figure 5.

Model 4b (below): Velocities were lowered in Tertiary and transition zones; the thrust zone was made more linear. The result is Figure 6.



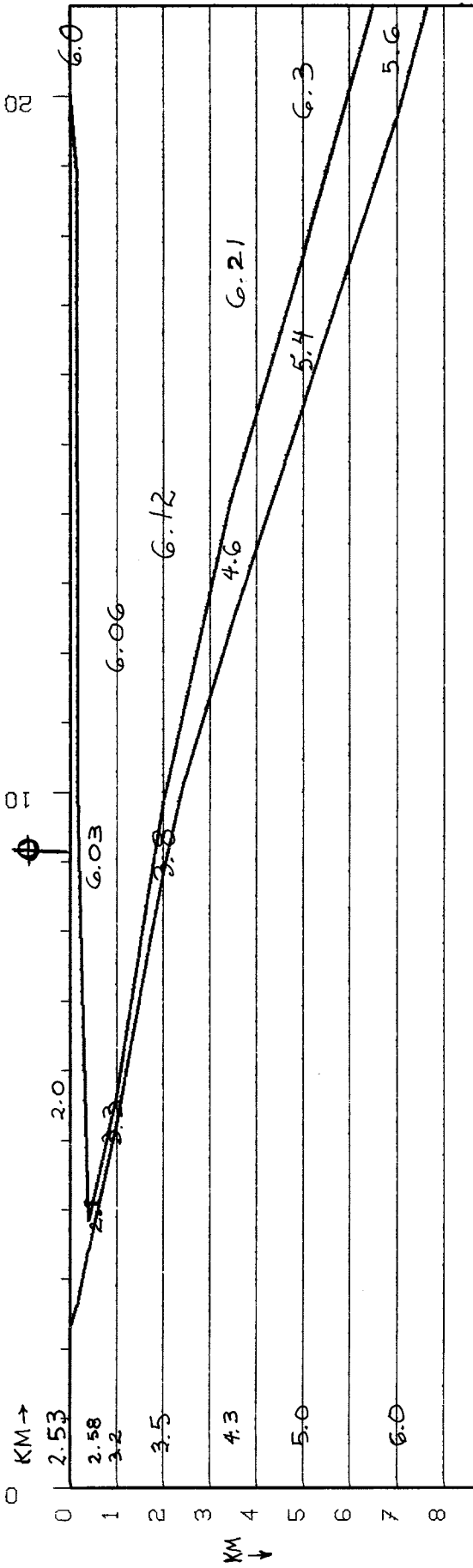
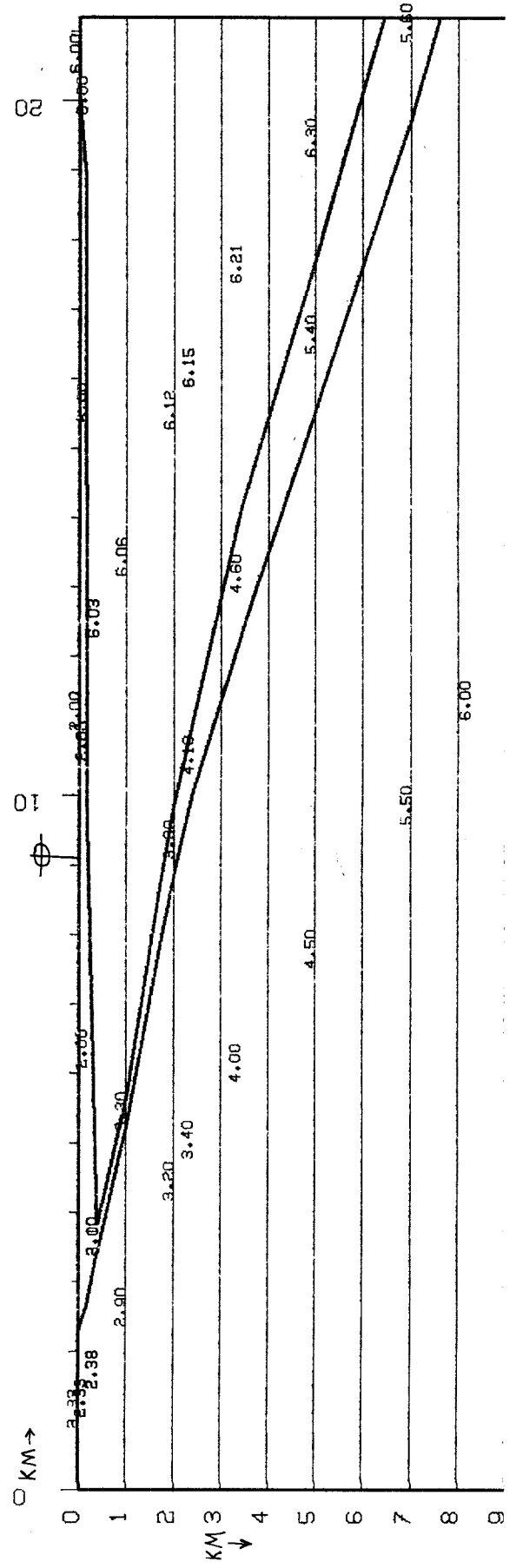


FIGURE 7.--Model 7a (above): The Tertiary sediment wedge was thickened as suggested by the unmigrated data; the fault zone was thinned with an accompanying thin Precambrian wedge. The result is Figure 8.

Model 7b (below): 8% slower velocities in the Mz sedimentary sequence than used in 7a; otherwise, 7b is identical to 7a. The result is Figure 9.



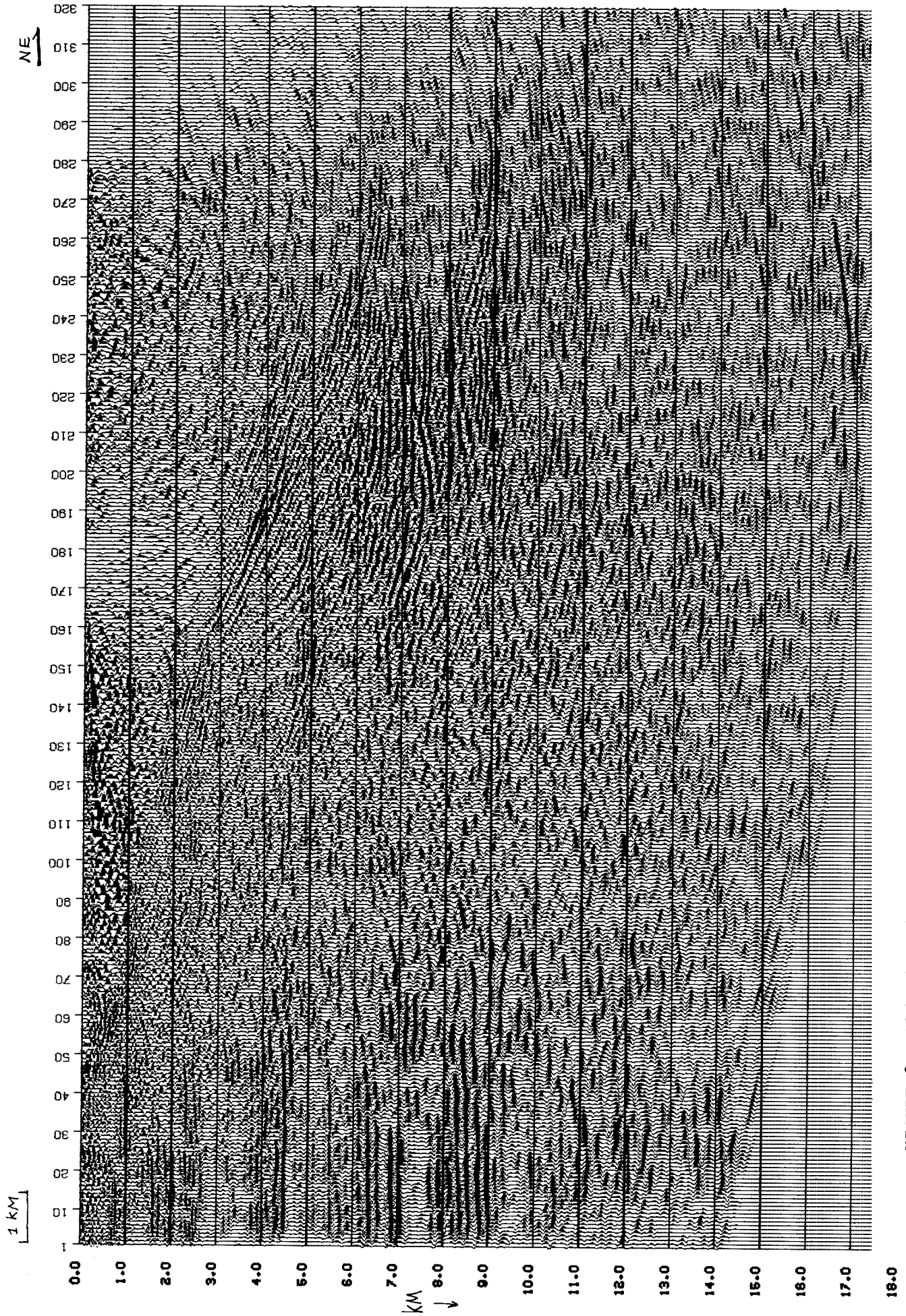


FIGURE 8.--This is a better migration than Figures 5 and 6. Fewer smiles are seen and their amplitudes are lower. Model 7a was input.

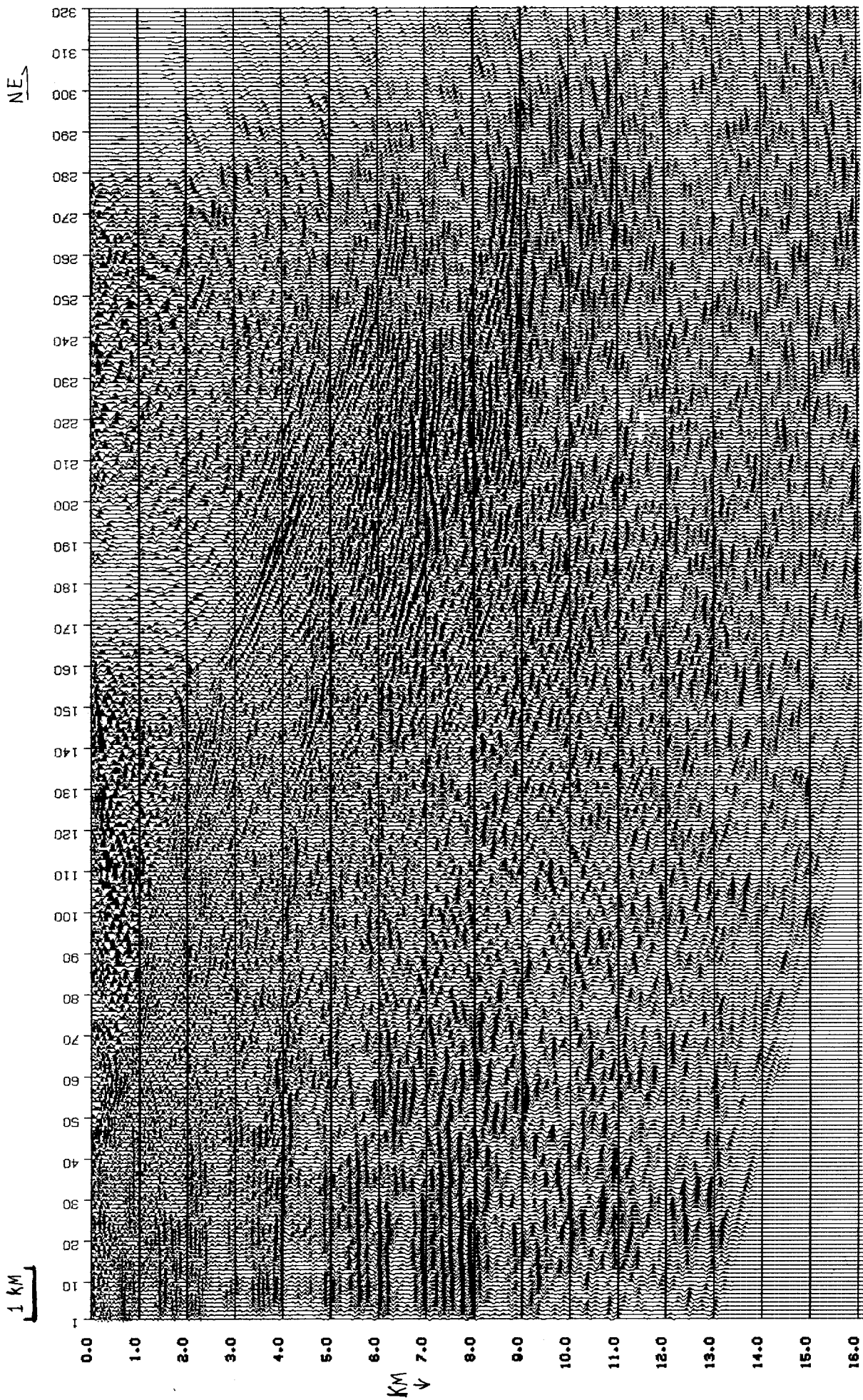


FIGURE 9.--This is a better migration than Figures 5-12. Very few overmigration or undermigration artifacts are seen. Model 7b was input (8% slower  $M_z$  velocities).

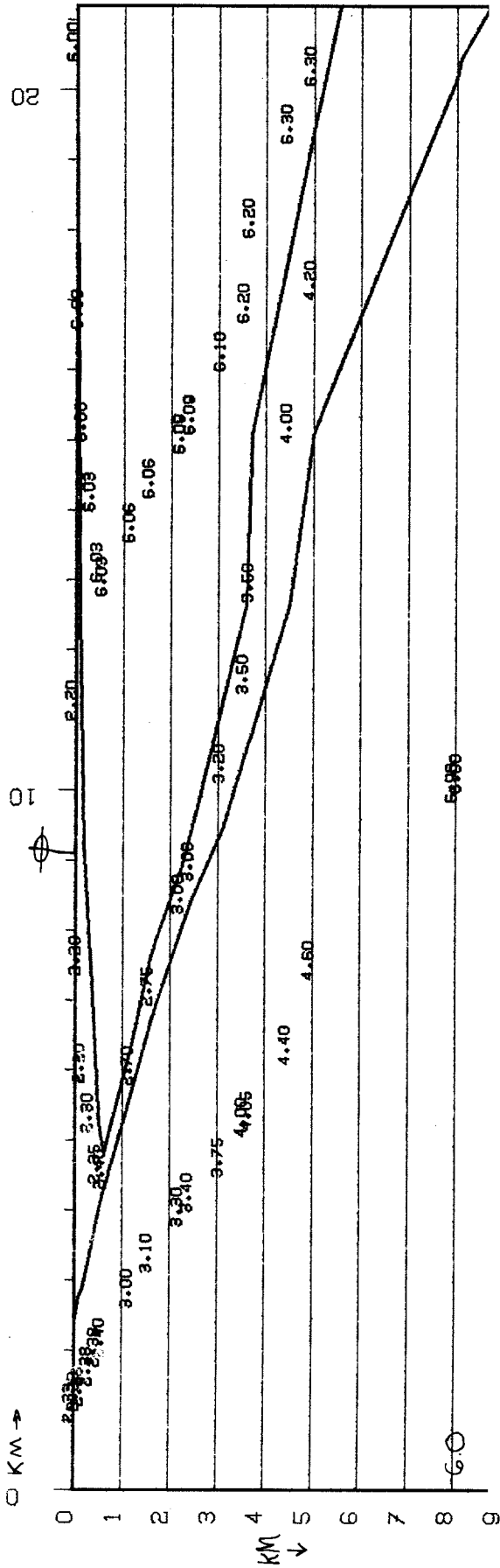


FIGURE 10.--Model 10a (above): Structure was taken from well data. Velocities of "fault zone" were testing the hypothesis that significantly lower velocities existed within the fractured Precambrian fault zone due to (possibly) water-filled pore space. The result is Figure 11.

Model 10b (below): From SEP-15, the best of the migrations (geologically-based) prior to well control. Note there is no Tertiary wedge (slow velocity), and the Precambrian velocity is 15% too slow. The result is Figure 13.

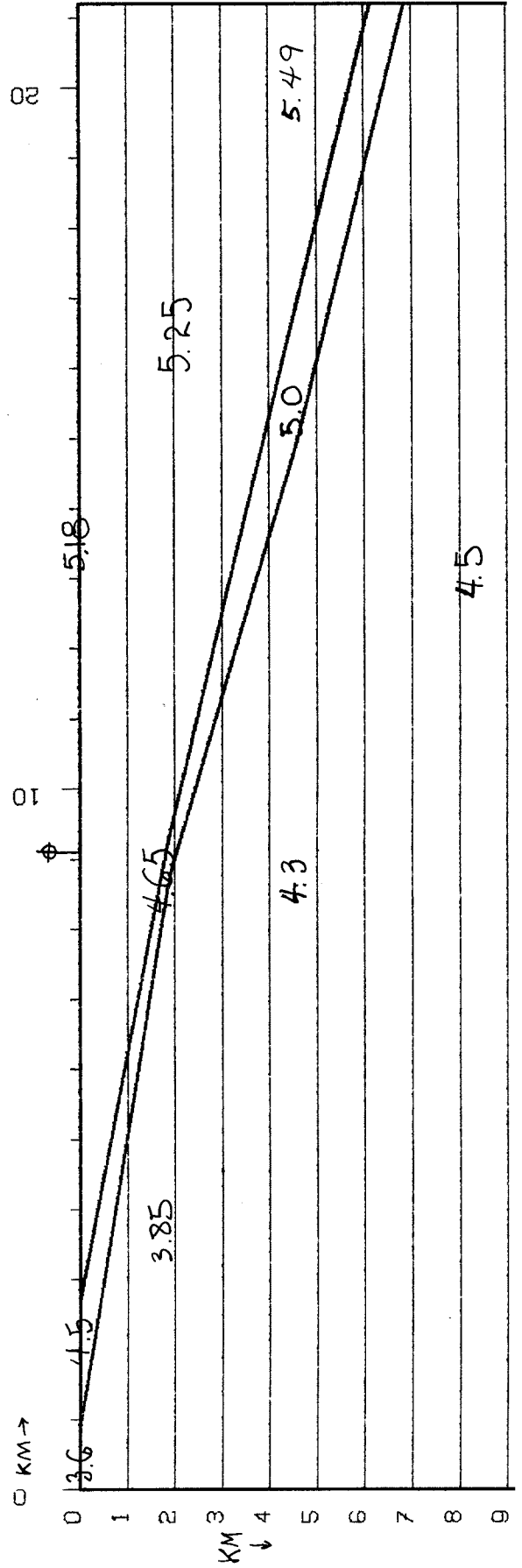




FIGURE 11.--Pullups in z ("smiles") are observed between traces 11 and 12, the conclusion is that these artifacts are due to too slow velocities in "fault zone." Model 10a was input.

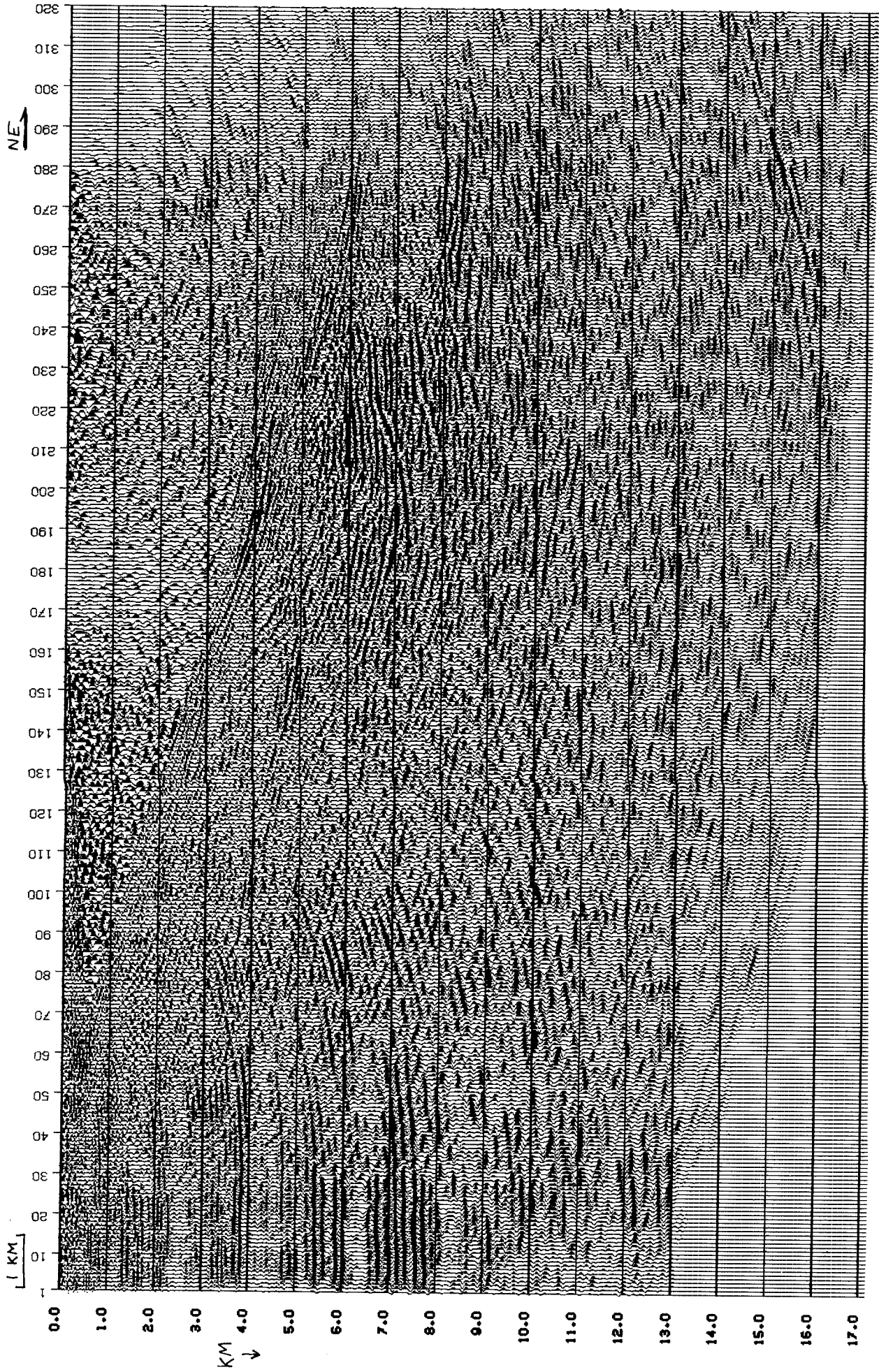


FIGURE 12.--Velocities were reduced 8% in the Mesozoic section, to see if overmigration of the sediments was causing "smiles." The artifacts are still observed, indicating that they are more likely pullups in z caused by too slow velocities in the "fault zone." The model used was identical to 10a, except that the velocities in the Mesozoic section (on the left) were 8% slower.

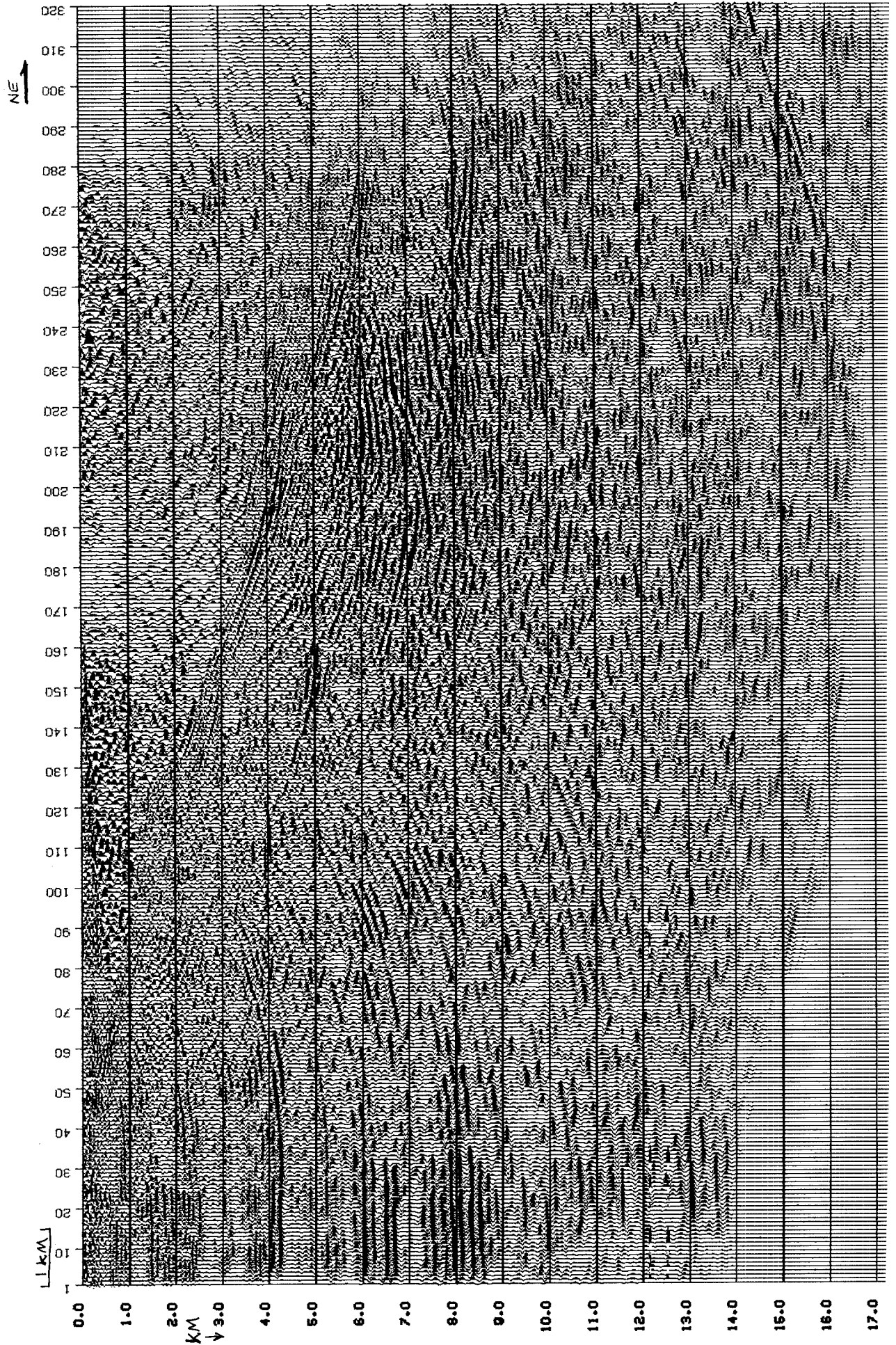
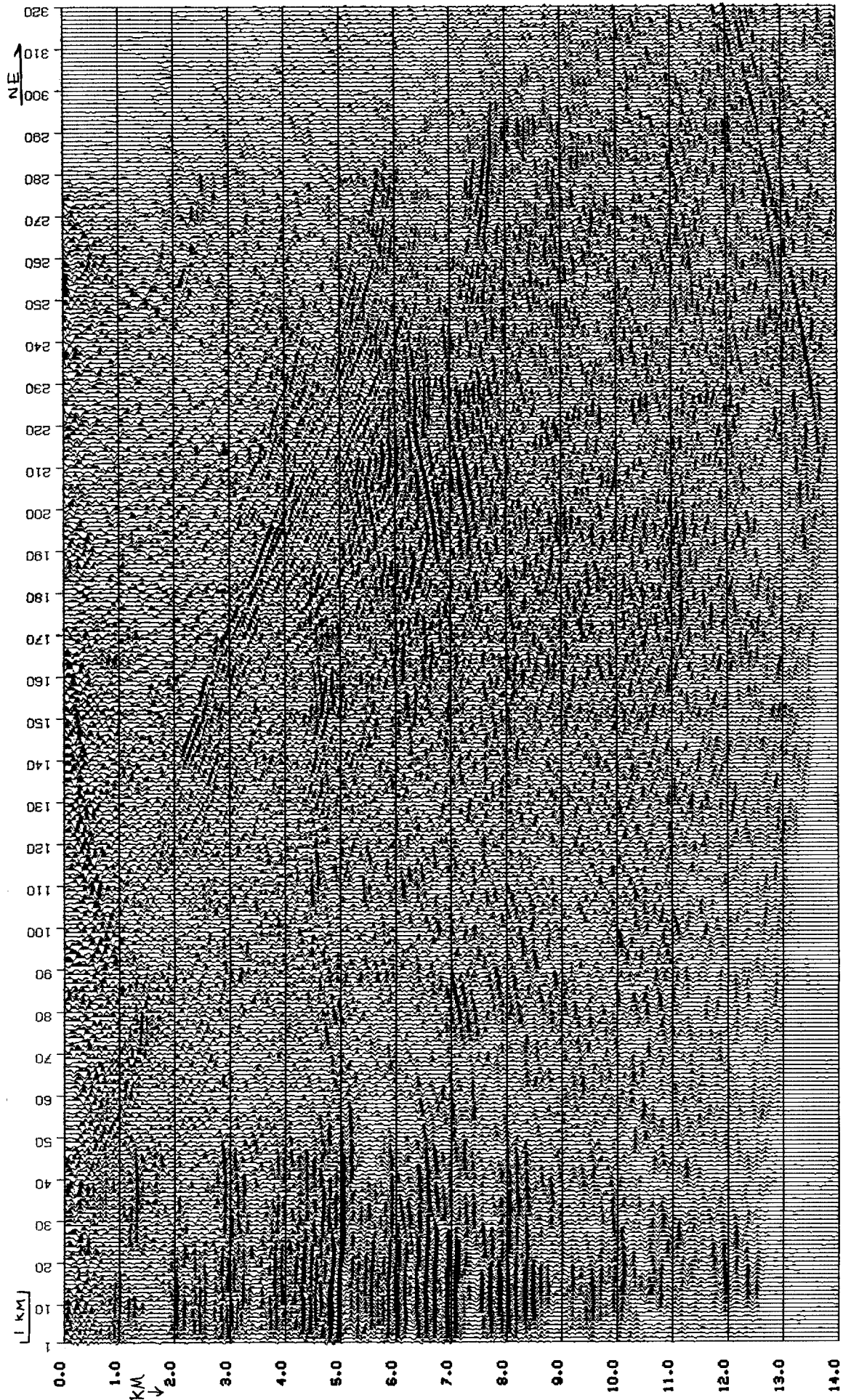


FIGURE 13.--The best of the migrations prior to well control (from SEP-15). The model used is Figure 10b. Note that the events at ~6.8 km (traces 20-50) are cut by energy which (in Figures 8 and 9) migrates up to the right, creating better reflector continuity in that area. This migration did not have dip filtering (viscosity), which was applied in later work, and so it appears more "ragged" or noisy. Model 10b was input.



brian fault zone, due to (water-filled) porosity. Therefore, velocities from 2.7 k/s at 1 km depth to 4.0 k/s at 4.5 km depth were chosen. Mesozoic sediment velocities were those used in the previous successful migration (Figure 7a and 7b).

Model 10a was used to make Figures 11 and 12. Figure 12 used 8% faster Mesozoic velocities. These two sections exhibit "smiles" suggestive of overmigrating the left-hand side Mesozoic sedimentary section. However, the smiles are attributed to the slower than correct velocities in the fault zone. The amount of reduction in velocities to test the above hypothesis is seen to be excessive. A more reasonable test would be half that amount of reduction.

Complicating the picture (both processing-wise and geologically) in all of the migrations is the extreme lateral velocity variation between traces 40-150, which degrades the CDP stack. Where reflectors would have been present on a true zero offset section, there are now "random holes" on the CDP stack. Unwanted "artifacts" may thus be produced in migration. Obviously, here a CDP stack does not approximate a zero offset section.

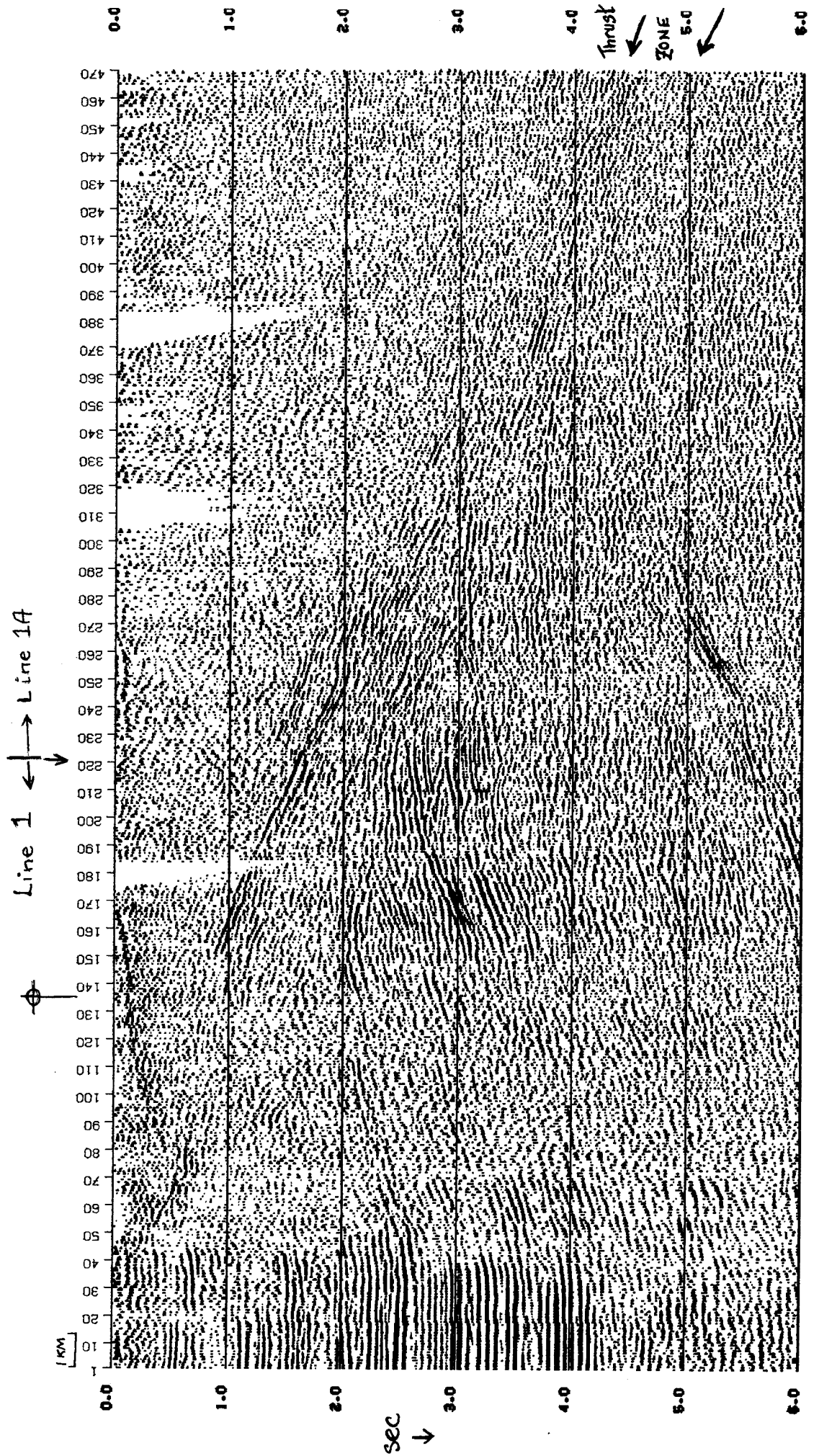
2) Comparison of "best migrations" to date with previous work. Figures 8 and 9 are considered better migrations than the migrations prior to access of well data (Figure 13). Figure 10b shows the model which made Figure 13 (both from SEP 15). In the new work, the Tertiary wedge is modeled, the Precambrian velocity is more accurate (i.e., higher), and the fault zone is more reasonably delineated. Note that the events at ~6.8 km on



Figure 13 are cut by energy which (in better migrations) migrates up to the right, creating better reflector continuity in that area. Also, on the older migration(s), the high amplitude event at 5.0 km (Figure 13, trace 1-50) is seen at 4.5 km depth under the thrust fault. Time pullup is still present, due to too slow Precambrian velocities. On newer migrations, however, the correlative event (Figure 8, 4.5 km, traces 1-50) continues on at 4.5-4.8 km depth. The Precambrian velocities were from ~6.0-6.1 km/s here, which are much better velocities. The conclusion is that the time pullup has been acceptably removed. (Whether the earth has been correctly imaged is a matter of interpretation.) Figure 13 may appear to some as being more noisy or "ragged"; the dip filter (viscosity) used in later work was not applied here.

3) Making of sections for geologic interpretation-- composite dataset migrations. For geologic interpretation, it was distressing to not see the fault trace below ~8 km on any of the migrations. Assuming that the reason was lack of input data, the dataset was increased by 50% laterally : a composite 470 trace (31.4 km) - 6 sec dataset from line 1 and line 1A was manufactured. The trace spacing of Line 1A was 50 m; it was resampled to be equal to Line 1's trace spacing of 67 m. Figure 14 shows the unmigrated composite time section (see basemap, Figure 1). Note that the fault reflection apparently continues down to 4.3 sec at the far right side. This energy will move up dip upon migration--we should then see a clearer delineation of geologic structure. Note that the large taper

FIGURE 14.--The composite 470-trace, 6-sec unmigrated time section made from line 1 and line 1A. (See Figure 1 for basemap location.) Trace spacing: 67 meters. Note arrows on right margin pointing to the thrust fault zone's reflections (~1.1 display).



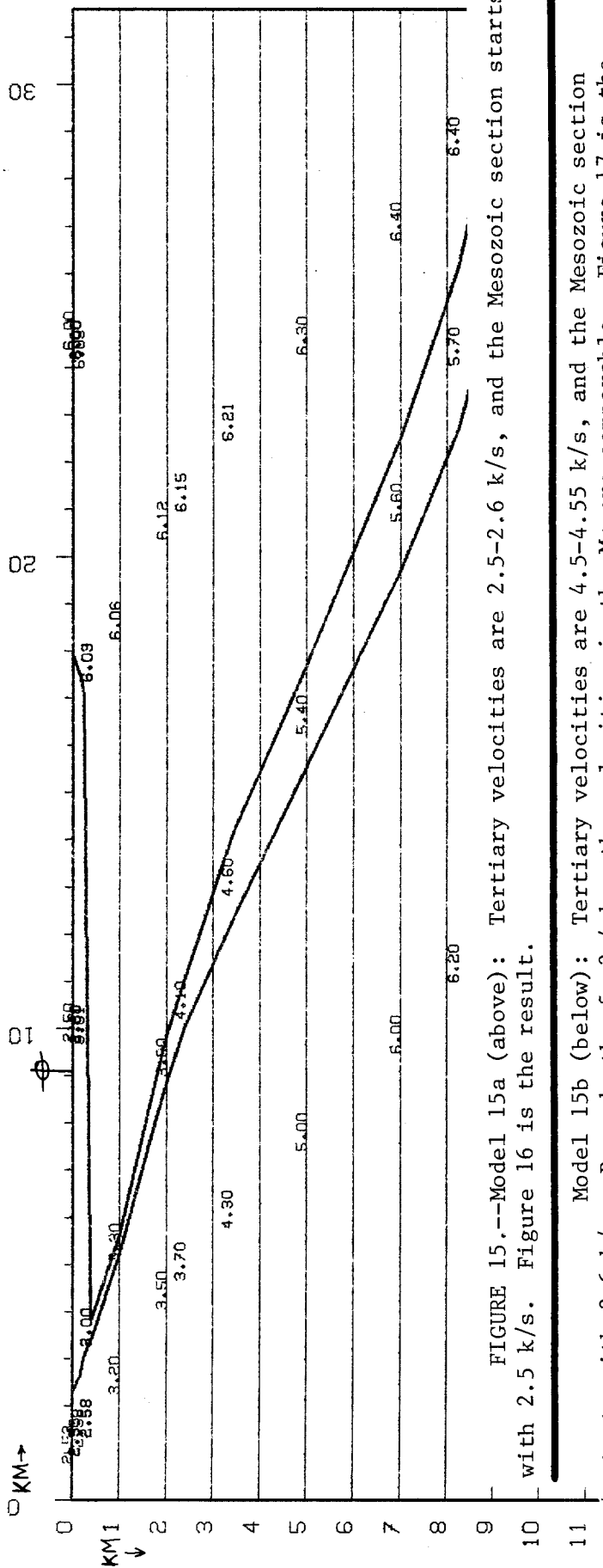
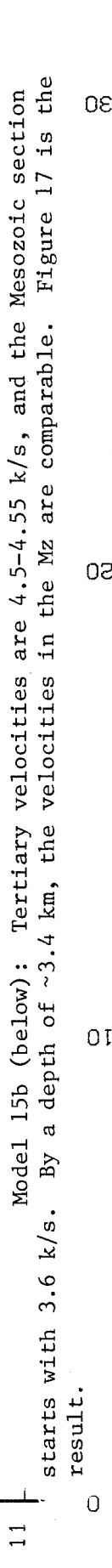


FIGURE 15.--Model 15a (above): Tertiary velocities are 2.5-2.6 k/s, and the Mesozoic section starts with 2.5 k/s. Figure 16 is the result.



Model 15b (below): Tertiary velocities are 4.5-4.55 k/s, and the Mesozoic section starts with 3.6 k/s. By a depth of ~3.4 km, the velocities in the Mz are comparable. Figure 17 is the result.

zone at the end of line 1 (Figure 2, traces 278-320) no longer exists.

The two models used were Figure 15a and 15b; the structure is the same, while the near surface velocities are somewhat different. Model 15a has Tertiary wedge velocities of 2.5 - 2.6 k/s; Model 15b, 4.5-4.55 k/s. Model 15a starts at the Mesozoic sequence with a lower velocity (2.5 k/s) than does Model 15b (3.6 k/s). By a depth of ~3.4 km, the velocities have become comparable. The resulting migrations are Figures 16 and 17, respectively.

Discussion of composite dataset migrations. The differences between Figures 16 and 17 are not obvious. They both show the Wind River thrust from 0 - ~12 km depth; deeper in the section, the thrust is difficult to find. The Mesozoic sediments appear to be acceptably imaged: there are few "smiles" or "frowns." In the Mesozoic sedimentary sequence under the thrust, the crosscutting energy, or superimposed dip segments, is interpreted to be real and to indicate imbricate (or subsidiary) thrusting at depth.

A difference between the two sections is seen from traces 20 -80, when comparing the high amplitude reflector at 7.5 km on Figure 16 with its counterpart on Figure 17 (at 8.0 km depth). On Figure 16, the three legged event (7.5 km, traces 50-70) has E-NE dip, while on Figure 17, the corresponding three legged event (8.0 km, traces 60-83) has opposite (W-SW) dip. As these dip segments are significantly high in amplitude, they would be used in any interpretation. Another more obvious



difference is the depth axis: the migration with the faster velocities (Figure 17) shows reflectors to be deeper in the earth. The velocities are not well enough known to place emphasis or confidence on the depths indicated after migration. (The depth is probably accurate to ~15%.) A thorough velocity analysis and restacking, assuming in both processes non-hyperbolic trajectories, are required before the post-migration depths can be trusted.

#### Geologic interpretation of composite dataset migrations

1) Elementary seismic interpretation techniques in thrust areas. Professionals working in these complex geologic areas have lectured on and published the basic seismic interpretation "maxims" they currently use. A few of the standard concepts they advocate are: (1) faults cut up section in direction of tectonic transport; (2) faults are parallel to bedding within incompetent rocks and are oblique to bedding within competent rocks (see Figure 18); (3) thrusts are known (recognized) by the interruption of stratigraphic sequence (layered reflectors); and (4) normal (extensional) faulting occurring after the major thrust faulting may occur and is seen in Wyoming, Utah, and Idaho, with the majority of such normal faults restricted to the thrust's hanging wall (Royce, 1979). Two dimensional seismic modeling of proposed interpretations in order to compare the match between observed and predicted is popular and useful, of course. Velocity pullup due to overthrust high velocity rocks is probably the most common "pitfall" observed

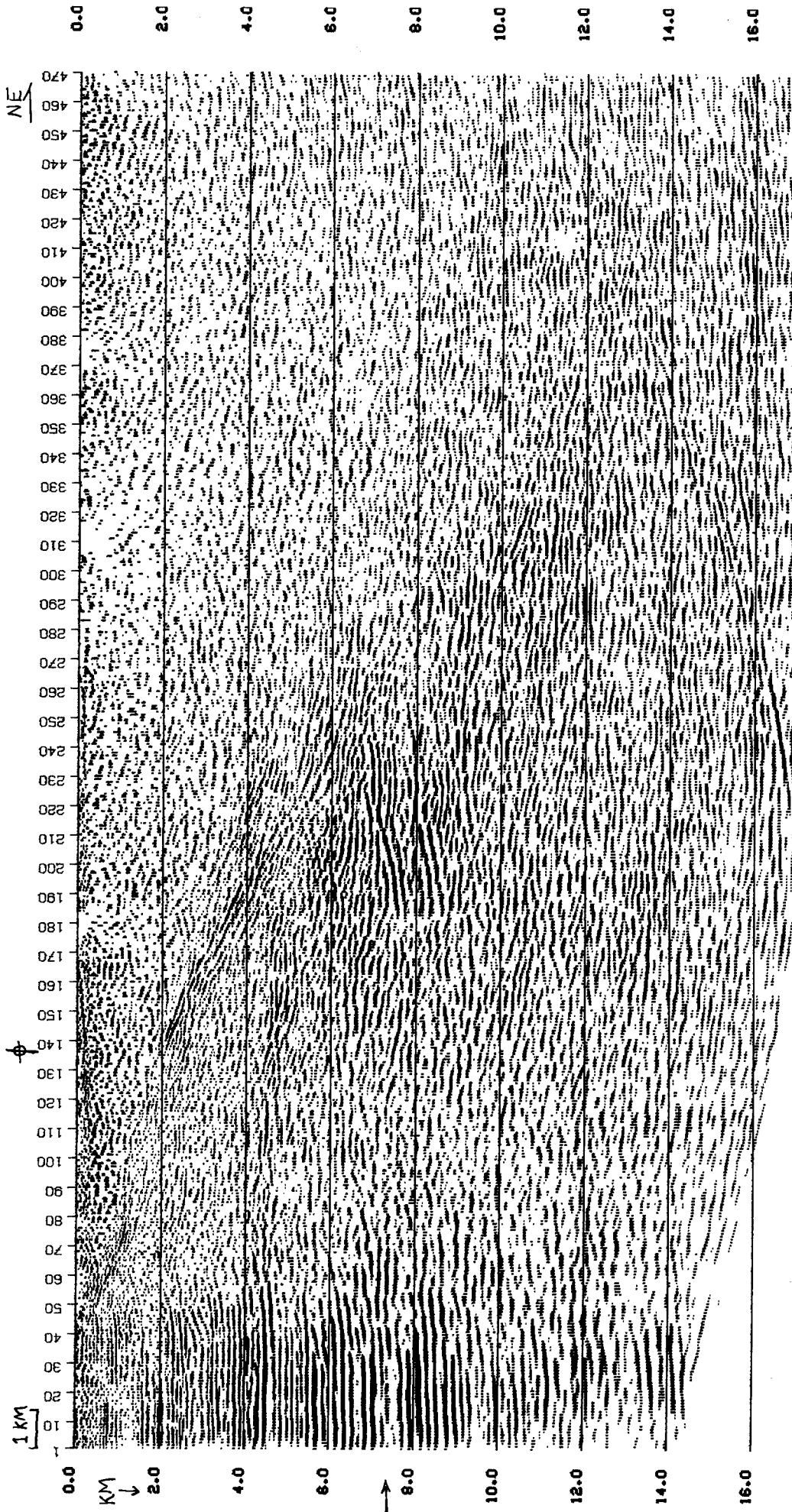
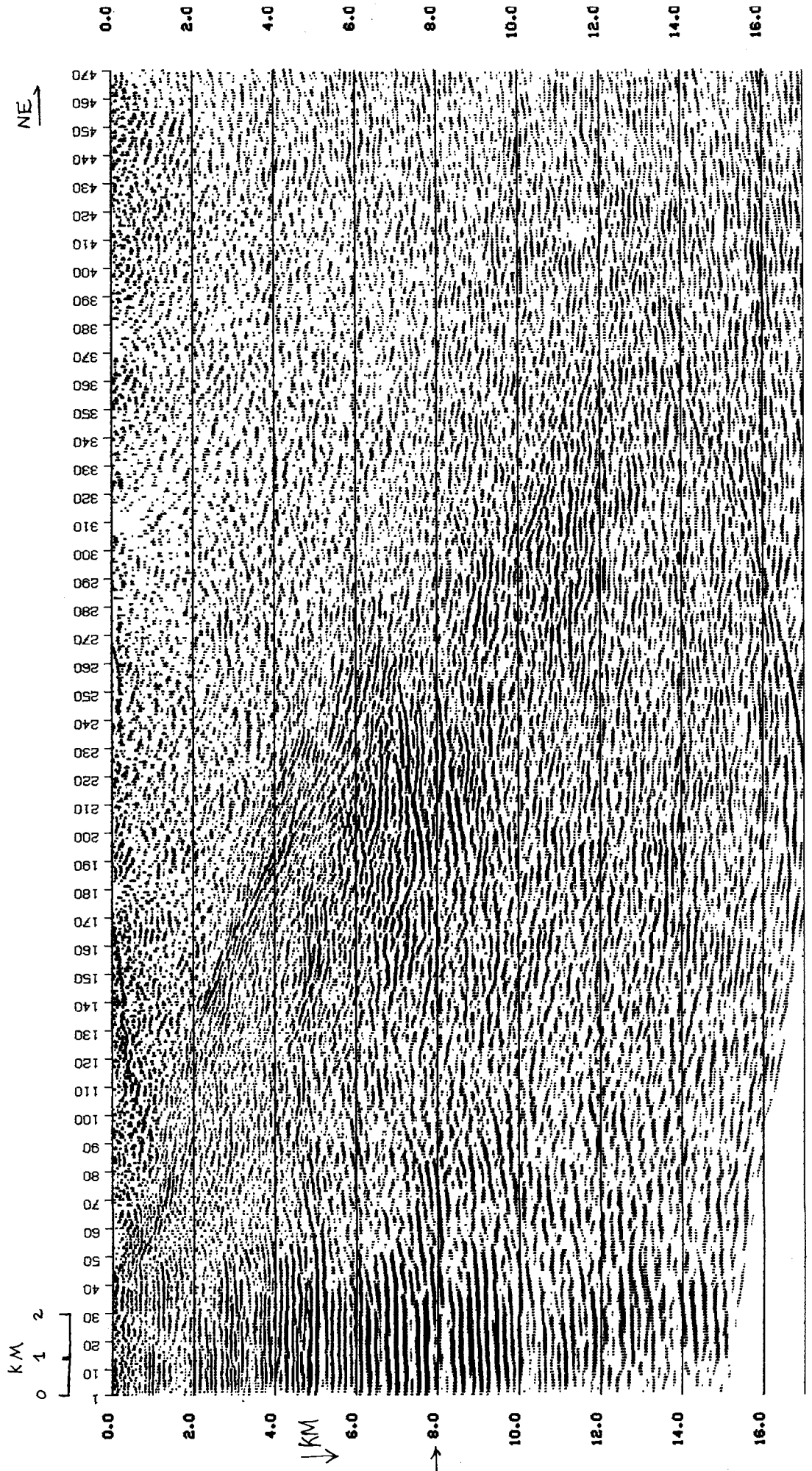


FIGURE 16.--Composite dataset migration (Figure 14 input). Model 15a was used. Note the "band" of higher amplitudes (along arrows) across the section; the band thickens at depth (10+ km). These reflections are interpreted to be from the Wind River thrust.

FIGURE 17.--Composite dataset migration (Figure 14 input). Model 15b was used. Note again the band of higher amplitude reflection along arrows (referred to in Figure 16). Note sharp delineation of Tertiary fill at the top of the section. Note cross-cutting dip segments on both Figures 16 and 17 in the Mz section under the thrust. These may be out of the plane of the section, or they may represent imbricate thrusting of depth (along bedding planes and oblique to bedding planes) as discussed in the text (Geologic Conclusions). (~1:1 display).



in thrust regions (see Figure 18). Nonetheless, Sacrisson (1978, Amoco Production Co.) writes that if the results of a careful velocity-study "are inconclusive, it may be less costly to drill a dry hole on a velocity anomaly than to miss an oil field."

Using all available geologic and structural information, and the fact that in this area thrusts are customarily interpreted by the divergence or overlapping of dip segments, Figure 17 was interpreted. Figure 19 is the line drawing illustrating our interpretation.

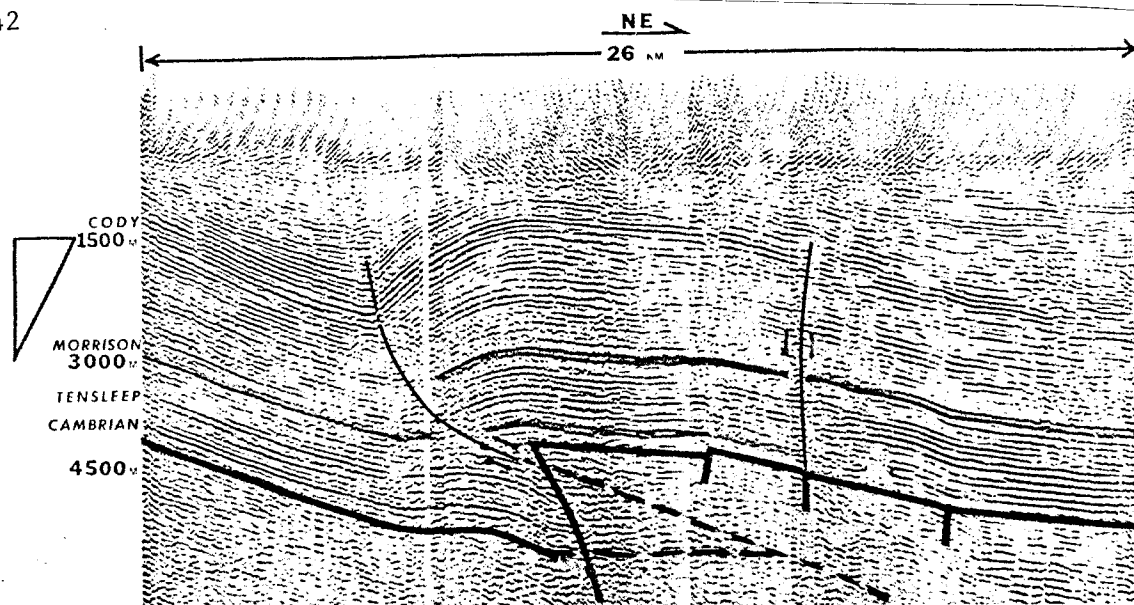
Upon close inspection of a large scale plot of Figure 17, it is observed that at the well's tiepoint, the top of the fault (fractured Precambrian rock) reflection is 250 m too shallow, thus indicating too slow velocities above it (either in the Tertiary or the Precambrian). However, when a match of the well's synthetic seismogram with the migrated data is obtained, the authors believe that this "correct migration" will look like the section (and interpretation) shown here.

#### Geologic conclusions

The thickness of the Wind River thrust zone as a function of depth may be estimated from the migrated data (Figure 17 and 19). The fault zone appears to be thin at and near the surface (50-250 m thick). However, reflections from within the Tertiary wedge to a depth of ~1.5 km may obscure or mask the fault zone's true thickness. At ~2.0 km depth, the fault zone appears to reach a local maximum thickness of ~750 m. At the well's tiepoint, the sonic log indicates the top of the 500 m

thick "low velocity fault zone" at ~2.5 km (or 2.74 km, depending on the interpreter; see Figure 2 and Table 3). The migrated section (Figure 17) shows a fault zone of ~500 m thick slightly shallower (2.25 km depth) at the well's tiepoint. A slight increase in dip angle coincides with a "thinning" of the fault zone to ~400 m at ~3 km depth. The seismic expression of the thrust zone widens with depth after that, to reach an (apparent) thickness of ~1.2 km at 5.5 km depth. Between 7 and 10 km depth (traces 270-290), there is a "gap" in the main thrust reflection; the subsidiary or imbricate thrusts in the sedimentary section are the more clearly delineated feature. At ~10 km depth, ~30 degree dipping energy (which is interpreted to be the Wind River thrust) is observed; the thrust zone may be as thick as 2 km at that depth. However, the upper reflection of the fault zone at these depths is not observed (see the dotted lines in Figure 18). This suggests: either (1) that the change in seismic impedance at the top of the fault zone is not sufficient to generate recordable energy, while the downthrown block's contact with the thrust zone does have a significant seismic impedance contrast; or, (2) that the interpretation should be that the Wind River thrust steepens between 6 and 10 km to ~45 degrees, and that we are observing the "top" of the thrust zone at 10.3 km at trace 300.

To postulate different reflection coefficients for the top and bottom of the fault zone is to postulate physical differences between the upthrown block's fault contact and the downthrown block's contact. Such differences are believed to be indicated by observed pore fluid distributions (Aydin, 1978;



Seismic section, southwestern Wind River Basin, Wyoming.

FIGURE 18.--Examples of seismic interpretation, Green and Wind River Basins, Wyoming (modified from Sacrisson, 1978).

Upper figure: Sacrisson states that these sections are unmigrated; however, the clarity of dip delineation here and the appearance of the first 100 m suggests a post-migration section. The "probable velocity pullup at the Tensleep and Cambrian horizons beneath the left side of the drape fold" is noted by Sacrisson. The dashed black line was drawn by Bloxson Lynn, suggesting an alternative interpretation more in accord with the deep seismic data recorded by COCORP in this area (and migrated by us).

Lower figure: Velocity pullup in the basement reflector under the Precambrian block is evident.

The triangles on the side indicate the average amount of vertical exaggeration. (Vertical exaggeration decreases with time on time sections as rock velocities increase with depth.)

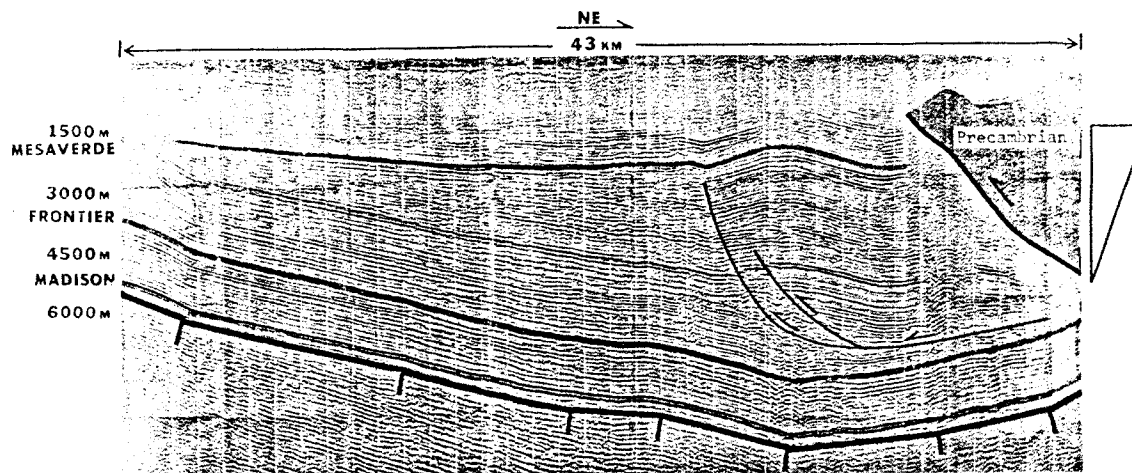


Figure 15. Seismic section, northern Green River Basin, Wyoming.

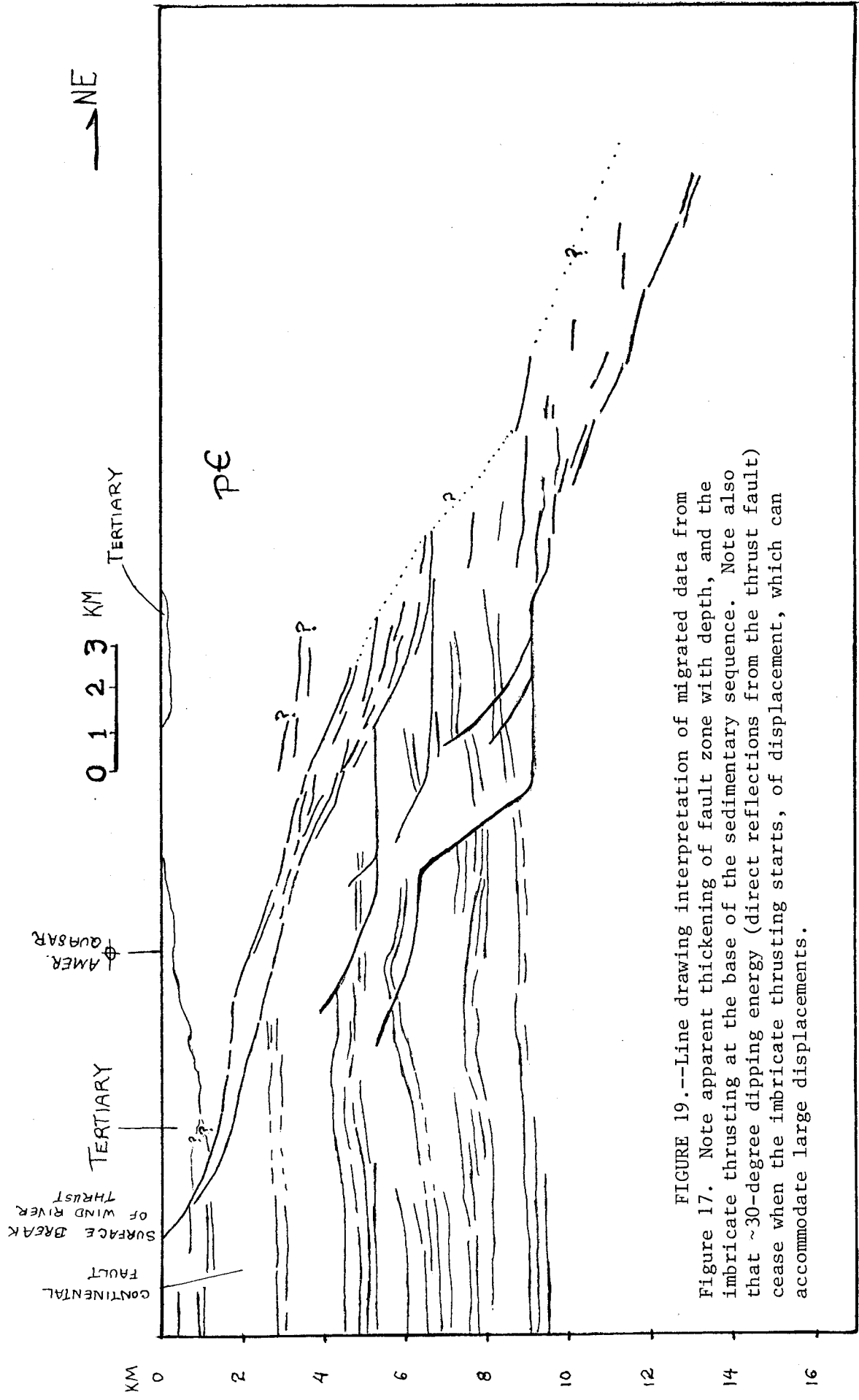


FIGURE 19.--Line drawing interpretation of migrated data from Figure 17. Note apparent thickening of fault zone with depth, and the imbricate thrusting at the base of the sedimentary sequence. Note also that ~30-degree dipping energy (direct reflections from the thrust fault) cease when the imbricate thrusting starts, of displacement, which can accommodate large displacements.

Weber et al., 1978; Thompson , 1966). One study of fault zones, based upon field observations in the Navajo and Entrada sandstones, southern Utah, found that shear deformation occurred in discrete zones with reduction of porosity and permeability within these zones (Aydin, 1978). With normal faulting, the slip plane <1> is found on one side or the other of the shear zone. In addition, the slip plane side of the shear zone may be dilatant or heavily fractured. Field observations here and in the Niger Delta suggest that the slip plane is generally found on the downthrown side of the shear zone. In the Niger Delta, the spillpoints of downthrown (hanging wall) reservoirs are at their contact with the fault (Weber et al., 1978). (These are normal faults.) Oil and gas migrate up along the porous-permeable fault contact. The upthrown (footwall) reservoirs are sealed next to the fault (probably) due to the low porosity and permeability of the fault zone. Here, normal faults provide poor barriers to fluid flow along downthrown blocks, and good barriers to flow along upthrown blocks. The upthrown block apparently does not face the slip plane, while the downthrown block does. The increased porosity associated with the slip plane can increase the reflection coefficient of the downthrown side of the fault zone and may be seen seismically if the slip "plane" is thick enough to affect a downgoing wave. So, if the fault zone is wide enough to see both its top

---

<sup>1</sup>Aydin (1977) defines a slip plane or slip surface as a through-going, locally planar surface of discontinuity of displacement, which can accommodate large displacements.



and bottom, this theory predicts that the bottom would have the larger amplitude reflection.

The application of this theory to the Wind River thrust proceeds thus: below 10 km only the bottom of the ~2 km thick fault zone is seen seismically. The lower block-- i.e., the downthrown block-- may face the slip plane, a zone of dislocation thick enough (~100 m) to be seen seismically.

The alternative to this theory is that between traces 265-300, the fault steepens to ~45 degrees from 7-10 km. Below 10 km, (the base of the sedimentary sequence), the thrust zone is seen as a zone of reflectors ~1 km thick.

Three substantial subsidiary thrust faults are seen in the sedimentary sequence between 5-10 km. Folding in the upper sedimentary horizons apparently preceded the faulting: sometimes the upthrust limb of a small severed anticline does not achieve a structurally higher position after thrusting. (See Figures 17 and 19, traces 145-190, ~5 km depth; and Fig. 20.)

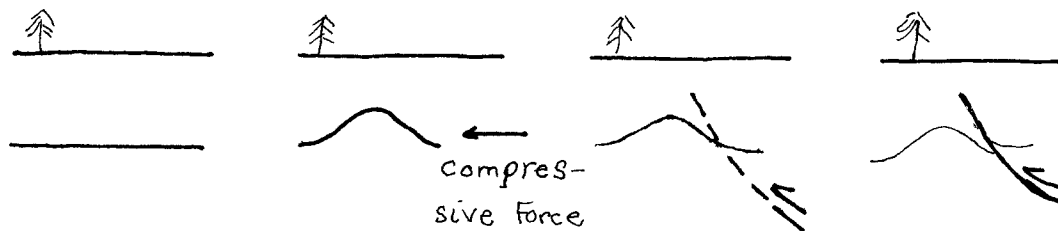


FIGURE 20.--Possible structural history resulting with the upthrust limb not achieving a structurally higher position after thrusting. This scenario implies folding prior to thrusting.

If an essentially flat horizon is thrust (as the lowest sedimentary reflector was), a structurally higher location of the thrust bed is usually seen. (See Figure 21.)

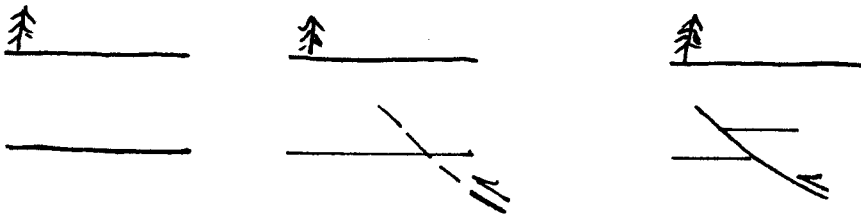


FIGURE 21.--Structural history resulting with the upthrust limb achieving a structurally higher position after thrusting.

At about 10 km depth (~traces 260-280) the thrust passes upward from Precambrian crystalline rocks to the sedimentary rocks of the Green River Basin. At this point, the angle of thrusting appears to change from ~30 degrees to ~0 degrees (slip along bedding planes). It is observed elsewhere in the Wyoming province that thrust faults are often parallel to bedding in less competent rocks and oblique to bedding in more competent rocks. Therefore, it is not surprising to have seismic data indicate that as the thrust leaves Precambrian crystalline basement at ~10 km, and enters the sedimentary layered (weaker) rocks, the thrust angle parallels bedding.

This change in the dip angle of the thrust fault also occurs at ~1.8 km (Figure 17). The thrust turns from 30 degrees to 0 degrees and parallels bedding (between trace 130 to 95),

faulting along the high amplitude reflector seen on the left side of the section at 1.8 km.

Upon examination of the unmigrated data (Figure 14), the change in the thrust angle at 10 km depth is indicated between 3.0-3.5 sec, traces 300-340. However, this observation required substantiation on a reasonably migrated section before advancing the hypothesis.

Presented above are our geologic hypotheses based upon the interpretation of the migrated data (Figure 17). As better migrations are produced, and more data on the Wind River thrust are uncovered, we hope to refine the interpretation. However, in the course of more than 25 different migrations on these datasets, certain common types of features have been noticed. These "blatant" reoccurring features are the ones discussed above. Of course, the better the migration, the clearer we hope to see the geologic structures. With "the" correct earth model, all the pieces should fall into place, within the limits of a two dimensional earth, dataset, and migration algorithm.

### Conclusions

A well close to our dataset in the Wind River Mountains, Wyoming, helped defined critical parameters in the  $V(x,z)$  model input to the 45 degree w-finite difference migration algorithm. Unfortunately, the seismic/sonic velocity estimates of a Tertiary wedge ranged between 1.8-4.0 km/s, thus introducing a considerable spectrum of possible migrations. Overmigration ("smiles") were produced when too fast velocities were used and undermigration "pullups in z" were produced when too slow velocities were used. The two best models were used to migrate a composite enlarged dataset. The best migrated sections allowed the estimation of the Wind River thrust zone thickness as a function of depth, the delineation of three subsidiary thrusts in the sedimentary sequence, and indicated a decrease in the thrust angle (30 degrees to 0 degrees) upon encountering the base of the sedimentary sequence.

### Acknowledgements

Rex Hanson and Pat Hart produced some migrations shown here and many others not shown. Einar Kjartansson wrote the 45 degree w-finite difference migration algorithm used herein; he also kindly and patiently solved the program problems we ran into. Walter Lynn wrote the spiffy plot program which displayed the  $V(x,z)$  earth models.

## REFERENCES

- AYDIN, A. (1977), "Analysis of faults as deformation bands, zones of deformation bands, and slip surfaces in porous sandstone," in *Faulting in Sandstone*, Ph.D. thesis, Chapter 4, Stanford University, to be published in *Tectonophysics*.
- HAYES, G. K. (1977), *Analysis and Interpretation of COCORP line 1, Wind River Uplift, Wyoming*, M.S. thesis, Geophysics Dept. (GE0610S), University of Houston.
- ROYCE, F. (Jan. 16, 1979), "Structural Geology of Western Wyoming - Northern Utah Thrust Belt and Its Relationship to Oil and Gas Accumulation," AAPG Distinguished Lecturer Tour, California State University at Hayward.
- SACRISSEON, W. R. (1978), "Seismic interpretation of basement block faults and associated deformation," in *Laramide Folding Associated with Basement Block Faulting in the Western U.S.*, V. Matthews, III, ed., *GSA Memoir 151*, pp. 39-50.
- THOMPSON, T. F. (1966), "San Jacinto Tunnel," in *Engineering Geol. in So. Calif.*, Los Angeles section, pp. 105-107.
- WEBER, K. J., G. MANDEL, W. F. TILAAAR, F. LEHNER, R. G. PRECIOUS (1978), "The role of faults in hydrocarbon migration and trapping in Nigerian growth fault structures," in *Proceedings of OTC Conferences*, pp. 2643-2653.

Addendum

The problem of the near surface Tertiary wedge's velocity has probably arisen from an internal inconsistency just observed. Data from the Quasar well was interpreted as showing the base of Tertiary at 500 feet (0.15 km), yet the Tertiary-Precambrian reflection was chosen at 0.167 sec (Figure 3, Table 3, Hayes, 1977). 0.167 sec corresponds with a depth of 1200 feet, according to the time-depth conversion given in Figure 3. Thus, an average velocity of 4.38 k/s is indicated for this 1200-foot zone. Tertiary velocities of 4.5-4.55 k/s were used in Model 15B: We stumbled onto these correct velocities trying to guestimate a "transition velocity" from Mesozoic sedimentary rocks (3.5-3.8 k/s) to Precambrian crystalline rocks (5.8-6.1 k/s). Model 15b has produced the best migration to date of the dataset (Figure 17). Before this internal inconsistency was observed, we had no satisfactory explanation as to why Model 15b (and Figure 17) worked so well and looked so good, using such high "Tertiary" velocities.

APPENDIX - *Field, recording, and processing parameters**Line 1. Wind River. Shot Oct.-Nov. '76.*

4 vibrator trucks used at all times.

32 geophones/station. Natural frequency - 7.5 Hz. Cables with 440 feet (134 meters) takeout spacing.

Recording system: MDS VIII. 48-channel with field summing and noise reject capability.

Number of channels - 48

Degree of stack - 2400% (nominal)

Channel spacing - 440 feet (134 meters)

Source spacing - 440 feet (134 meters)

Digitizing rate - 8 milliseconds

Sweep frequencies - 8 to 32 Hz

Number of sweeps per record - 16

Sweep duration - 25 seconds

Total sweep time per record - 6-2/3 minutes

Record time - 50 seconds

Filters:

Low-pass: Anti-alias for 8 milliseconds (31.25 Hz)

High-pass: Butterworth type.  $f_0 = 9$  Hz with attenuation rate of 24 decibels per octave.

(Reference sweep used for correlation was recorded through above filters.)

Spatial filters:

Geophone array: 32 geophones configured to an in-line array symmetrical about its center. Elements equally sensitive, with spatial distribution of elements according to (Petty-Ray) VADIS equation. Array oriented radial to source. Length = 600 ft (183 m).

*Line 1A. Wind River. Shot Oct. '77.*

4 vibrator trucks used at all times.

24 geophones/trace. Natural frequency - 7.5 Hz

Recording system: MDS-10. 96-channel with field summing and noise reject capability.

Number of channels - 96

Degree of stack - 2400% (nominal)

Channel spacing - 330 feet

Source spacing - 660 feet

Digitizing rate - 8 milliseconds

Sweep frequency - 8 to 32 Hz

Number of sweeps per record - 16

Sweep duration - 30 seconds

Record time - 50 seconds

Filters:

Low-pass: Anti-alias for 8 milliseconds (31.25 Hz)

High-pass: Out

Spatial filters:

Geophone array: 24 EV-22 B 7.5 Hz geophones were used in an in-line array. All the elements of equal sensitivity were spaced 28.7 feet on the ground to provide total array length of 660 feet.

Identical source array for lines 1, 1A: Four or five vibrators in-line, spaced 88 feet (26.8 m) apart. Move up per sweep: 29-1/3 feet (8.9 m). Sixteen summed sweeps per records.

Four unit array - 704 feet long. Five-unit (vibrating trucks) array - 792 feet: The four-unit array had a length of 704 feet with 25 elements equally spaced with weighting:

1112223334444444333222111

The five-unit array was 792 feet long with 28 elements, equally spaced, with weighting:

1112223334445555444333222111

*Processing procedures*

The data were processed by the Houston data processing center of Geosource Inc. The processing was done using the TEMPUS computer and associated software. The programs utilized by this system were developed by Geosource for seismic data processing. The following basic processing was used for the COCORP data in Wyoming.

1. Demultiplex of field data (DEMUX)
2. Vibroseis Correlation (VIBCOR)
3. CDP Sort (static corrections applied)
4. Digital AGC
5. Velocity analyses (VELSTACK & Constant Velocity Stacks)
6. Normal Moveout Corrections
7. Trace Suppression (MUTE)
8. Automatic Residual Static Corrections (ARSTAT)
9. Common Depth Point Stack (2400% CDP nominal)
10. Deconvolution
11. Digital Filter
12. Digital AGC
13. Photo Display

(from Geosource Exploration Services Division, Houston, Texas)